American Mineralogist, Volume 63, pages 1190–1197, 1978

Lattice dynamical study of the α-β quartz phase transition

KAZUAKI IISHI[1]

Mineralogisches Institut der Technischen Universität Hannover
Hannover, West Germany

Abstract

The frequencies of the phonon spectrum at zero wave vector, the contribution of the various model potential terms to potential energy, the dielectric constants, and the mode oscillator strengths of quartz at 25, 580 and 600°C have been calculated from a polarizable ion model. The mode softening of the soft mode is attributable to the change of the contribution of potential energy terms to potential energy. The elastic constants, the contribution of potential terms to the elastic constants, and the change of internal coordinates due to the elastic stress have also been calculated. The anomalous elastic behavior near the transition point results both from the unusually negative contribution of the short-range internal rotation forces to the elastic constants at 580°C and from the rather large contribution of the strong short-range stretching forces at 600°C.

Introduction

The long-range Coulomb interactions were first applied to the lattice-dynamical theory of α quartz by Elcombe (1967) who calculated the optical mode frequencies and the phonon dispersion curves on the basis of the rigid ion (RI) model. The effective charge of the oxygen ion was $-0.98e$. The most elaborate and consistent lattice-dynamical theory of α quartz was presented by Striefler and Barsch (1975) on the basis of the modified RI model. The effective charge of the oxygen ion obtained by them is $-0.475e$ and is very different from that obtained by Elcombe. Both calculations neglected the electronic polarizability of the oxygen ion, which may be expected to play an important role in the long-range Coulomb interactions. Iishi (1976) studied the effects of the electronic polarizability of the oxygen ion on the lattice dynamics of α quartz and found that the fit to the experimental *TO–LO* splitting is improved by their inclusion. However, no attempt was made to examine the validity of the calculated electronic polarizability by comparison with the calculated and observed dielectric constants. Thus the first purpose of this paper is to reexamine the electronic polarizability and the effective charge of ions in quartz on the basis of a polarizable ion (PI) model.

From the work on the Raman spectrum of quartz from 6 to 900°C, Scott (1968) and Höchli and Scott (1971) presented evidence that the 207cm^{-1} A_1^4 mode is a soft mode. By analogy with several ferroelectric phase changes, Coulomb interactions must play an important role in the softening of the soft mode. For this reason, the second purpose of this paper is to clarify the effect of the Coulomb interactions on the softening of the soft mode in the α–β quartz phase transition.

Some of the elastic constants of quartz have an abnormally sharp decrease at the transition point. Yamamoto (1974) interpreted this abnormal behavior qualitatively by considering the contribution from the soft branch as a deviation from the Landau theory of phase transitions. Axe and Shirane (1970) showed that the critical softening of elastic constants of β quartz can be explained in terms of anharmonic interaction between soft and acoustic modes. However, nobody appears to have explained this problem by actual numerical calculation. Thus the third purpose of this paper is to give a quantitative and microscopic interpretation for this abnormal behavior by numerical calculation of both the elastic constants and the optical mode frequencies of quartz at 25, 580, and 600°C.

[1] On leave from the Department of Mineralogical Sciences, Faculty of Literature and Science, Yamaguchi University, Yamaguchi, 753 Japan (present address), with support from the Alexander von Humboldt Foundation.

0003-004X/78/1112-1190$02.00

Method of calculation

The structure and symmetry properties of quartz were described by Barron *et al.* (1976). The lattice dynamical calculation was performed using a space group $P3_221$ for α quartz and $P6_222$ for β quartz. The temperature variation of the unit-cell dimensions is taken from Jay (1933): $a = 4.9128$ and $c = 5.4045$A at 25°C; $a = 4.9962$ and $c = 5.457$A at 580°C; and $a = 4.9979$ and $c = 5.4582$A at 600°C. The temperature dependence of the atomic parameters is taken from Young (1962): $x = 0.4152$, $y = 0.2678$, $z = 0.1184$, and $u = 0.4705$ at 25°C; $x = 0.4153$, $y = 0.2133$, $z = 0.1527$, and $u = 0.4922$ at 580°C; and $x = 0.4137$, $y = 0.2068$, $z = 0.1667$, and $u = 0.5$ at 600°C.

The temperature dependence of the infrared active *TO* and *LO* frequencies and that of the oscillator strengths of α and β quartz are taken from Gervais and Piriou (1975), and those of the far infrared region from Russel and Bell (1967). The temperature dependence of the Raman active optical frequencies is taken from Scott and Porto (1967), Bates and Quist (1972), and Höchli and Scott (1971). The temperature dependence of the elastic constants is taken from Atanasoff and Hart (1941) and Kammer *et al.* (1948). The temperature dependence of the high-frequency dielectric constants is obtained by squaring the observed refractive indices. The static dielectric constants of α quartz are taken from Bechmann (1958).

A group theoretical analysis may be carried out on the symmetry properties of the normal modes of vibrations, and the dynamical matrices can be factorized into block matrices using **U** matrices (Chen, 1967). In this study, the matrices **U** are chosen both to satisfy the *0x* diad axis (Barron *et al.*, 1976) for the doubly degenerate modes E of α quartz and E_1 and E_2 of β quartz, and to destroy this two-fold symmetry for E' of α quartz and E_1' and E_2' of β quartz.

The method of PI model calculations of optically-active vibration frequencies of ionic crystals was described by Yamamoto *et al.* (1976). Aspects of the PI model relevant to the present work are briefly given here.

From Born and Huang (1954), a dynamical matrix **D** is constructed by four constituents in the form

$$\mathbf{D} = \overline{\mathbf{M}}(\mathbf{F}^N + \mathbf{F}^C + \mathbf{F}^I + \mathbf{F}^M)\overline{\mathbf{M}}$$

where the notations are those of Yamamoto *et al.* (1976) and $\overline{\mathbf{M}}$ denotes the inverse-mass matrix. The first term arises from short-range non-Coulomb interactions. The second is the Coulomb interaction part due to the undeformable ion interactions. The third is the Coulomb interaction part resulting from the induced dipole interactions through the electronic polarizability. The last term refers to the macroscopic field and is dependent on the direction of the propagation, whereas the first three terms are independent of the direction of the wave propagation in the long-wavelength limit.

The modified Urey-Bradley force field (Shimanouchi, 1963), which is used in the calculation of the non-Coulomb interaction part $\mathbf{F}^N$, contains the Si–O stretching force K, the non-bonded O···O repulsive force F, the Si–Si interactions between neighboring Si atoms to stabilize the Si–O–Si angles f, and the three correction terms of the internal rotation force Y, the intramolecular tension κ for the SiO_4 tetrahedron, and the bond–bond interaction force p for the adjacent Si–O bond pairs.

The Coulomb contribution can be calculated by means of Ewald's (1921) method. The effective charge of an oxygen ion Z_O is taken to be $-Ze$, where Z is a positive number. The charge of a silicon ion is obtained under the condition that the crystal is electrically neutral.

The high-frequency dielectric constants ϵ^∞, which are useful to check the validity of the chosen electronic polarizability values, can be evaluated in the form (Born and Huang, 1954)

$$\epsilon^\infty = \mathbf{I}' + 4\pi v^{-1}\boldsymbol{\rho}$$

where

$$\mathbf{I}'_{\alpha\beta} = \delta_{\alpha\beta}$$

$$\rho_{\alpha\beta} = \sum_{kk'} \mathbf{R}_{\alpha\beta kk'}$$

$$\mathbf{R} = (\mathbf{I} - \mathbf{AQ})^{-1}\mathbf{A}$$

$$\mathbf{A}_{\alpha\beta kk'} = \delta_{kk'}\alpha_{\alpha\beta k}$$

$$\mathbf{I}_{\alpha\beta kk'} = \delta_{\alpha\beta}\delta_{kk'}$$

The notations are those of Yamamoto *et al.* (1976). v is the unit-cell volume, **Q** the Coulomb coefficient matrix and α_k the electronic polarizability tensor of the kth atom. The static dielectric constants ϵ^0 are given by (Born and Huang, 1954)

$$\boldsymbol{\epsilon}^0 = \boldsymbol{\epsilon}^\infty + 4\pi v^{-1}[\sum_{t}\sum_{kk'}\{(\tilde{\mathbf{S}}\mathbf{M}_z)\mathbf{X}_{ti}\boldsymbol{\Lambda}_{ti}\tilde{\mathbf{X}}_{ti}(\mathbf{M}_z\mathbf{S})\}_{kk'} + \boldsymbol{\rho}]$$

$$= \boldsymbol{\epsilon}^\infty + \sum_j \Delta\boldsymbol{\epsilon}_j$$

where

$$\mathbf{M}_{z\alpha\beta kk'} = \delta_{\alpha\beta}\delta_{kk'}\mathbf{Z}_k\mathbf{m}_k^{-1/2}$$

$$\boldsymbol{\Lambda}_{t\alpha\beta l} = \delta_{\alpha\beta}\boldsymbol{\lambda}_{tl}$$

$$\mathbf{S} = \mathbf{I} + (\mathbf{I} - \mathbf{AQ})^{-1}\mathbf{A}$$

Table 1. Experimental and theoretical optical mode frequencies (in cm^{-1}) and high-frequency dielectric constants of quartz at 25, 580, and 600°C based on the PI model

Species		Experimental 25°C[a]	Experimental 580°C[b]	Species		Experimental 600°C[b]	Theoretical 25°C S & B[c]	Theoretical 25°C Present work	Theoretical 580°C Present work	Theoretical 600°C Present work
A_1	1	1085	1072	B_1	1	(1072)[d]	1127.3	1095.9	1101.1	1090.7
	2	464	464	A_1	1	464	474.1	487.4	463.8	465.9
	3	356	350	B_1	2	(350)[d]	375.0	352.8	336.7	341.9
	4	207	43[e]	B_1	3	(30)[d,e]	203.9	210.4	43.0	30.9
A_{2T}	1	1071	1064.5	A_{2T}	1	1061	1134.7	1073.0	1053.9	1067.4
	2	777	777	B_{2T}	1	(777)[d]	745.7	783.1	752.0	748.7
	3	495	436.5	A_{2T}	2	435	531.4	504.4	445.2	439.9
	4	363.5	385	B_{2T}	2	(385)[d]	379.8	358.8	408.8	419.8
A_{2L}	1	1229	1230	A_{2L}	1	1227	1153.4	1135.2	1126.4	1127.0
	2	790	781	B_{2L}	1		754.8	784.7	752.4	
	3	551.5	528	A_{2L}	2	527	545.5	504.5	445.2	439.7
	4	386.7	397	B_{2L}	2		388.0	358.9	408.1	
E_T	1	1158	1155	E_{2T}	1	1155	1086.9[f]	1092.1	1162.0	1161.9
	2	1065	1060	E_{1T}	1	1057	1135.2[f]	1071.8	1059.9	1056.6
	3	797	781.5	E_{1T}	2	779	775.0	795.3	780.5	783.1
	4	695	680	E_{2T}	2	680	667.9	691.1	667.7	669.1
	5	450	421.5	E_{1T}	3	420	494.6	457.6	429.6	428.0
	6	393.5	400	E_{2T}	3	400	378.0	380.2	359.2	361.1
	7	265	243	E_{2T}	4	243	256.2	257.9	255.7	255.0
	8	128	98	E_{1T}	4	98	136.3	128.1	94.8	94.8
E_L	1	1155	1154	E_{2L}	1		1154.2	1092.0	1162.0	
	2	1226	1228	E_{1L}	1	1223	1086.9	1131.3	1127.5	1116.5
	3	810	797	E_{1L}	2	796.5	784.0	797.2	782.6	785.1
	4	697.6	681	E_{2L}	2		668.5	691.2	668.0	
	5	510	494.5	E_{1L}	3	492	511.5	457.8	429.7	428.3
	6	402	403.7	E_{2L}	3		380.6	380.3	359.3	
	7	265	243	E_{2L}	4		256.9	258.2	255.8	
	8	128	98	E_{1L}	4	98	136.4	128.2	95.2	94.8
ε_1^∞		2.386	2.350			2.353	1.0	2.392	2.346	2.357
ε_{II}^∞		2.415	2.373			2.377	1.0	2.413	2.359	2.377

a: Data are from Gervais & Piriou (1975), except A_1 modes data which are from Scott & Porto (1967).
b: Data are from Gervais & Piriou, except A_1 modes and the two lowest E modes data which are from Bates & Quist (1972). *c: Striefler & Barsch (1975).* *d: These values are used for a least-squares fit analysis.*
e: These values are estimated from Fig. 1 of Höchli & Scott (1971). *f: Corrected assignment. From the magnitude of obtained TO-LO splittings by them, their assignment seems to be wrong.*

The subscript t identifies the transverse mode, and the summation with respect to i is extended over the infrared active modes. $\mathbf{X}$ is the atomic displacement of the normal mode of vibration, λ the eigenvalue, and $\Delta\epsilon_j$ the oscillator strength of the jth vibration. The first term, ϵ^∞, is the contribution of the ultravio-

Table 2. Parameter values of quartz at 25, 580, and 600°C in the best-fitting PI model

Parameter	Units	25°C	580°C	600°C
K	mdyn/Å	4.6696	4.9606	4.9666
F	mdyn/Å	0.6409	0.5461	0.5409
f	mdyn/Å	0.4820	0.5192	0.5224
Y	mdyn·Å	0.0011	0.0005	0.0032
κ	mdyn·Å	0.2024	0.2348	0.2462
p	mdyn/Å	-0.3708	-0.0391	-0.0026
Z_O	e	-0.349	-0.335	-0.335
$\alpha_\perp(O)$	Å^3	1.37	1.37	1.37
$\alpha_{/\!/}(O)$	Å^3	1.38	1.38	1.38
χ^*	%	1.69**	2.52	2.56

* *Longitudinal optical mode frequencies are not included in the quality-of fit parameter.*

** *Striefler & Barsch's model has the value 4.86.*

let and the second, $\Sigma_j \Delta\epsilon_j$, of the infrared polarization.

The elastic constant has been calculated by the method established by Shiro and Miyazawa (1971). The contribution of the potential term to the elastic constant $(\mathrm{PED})^E_{i,j,h}$ and the change in the internal coordinates due to the elastic stress have also been calculated by the method of Yamamoto *et al.* (1974a). The short-range parameters based on a short-range (SR) model have been refined by the least-squares fit both to the observed optical mode frequencies and to elastic constants (Yamamoto *et al.*, 1974b).

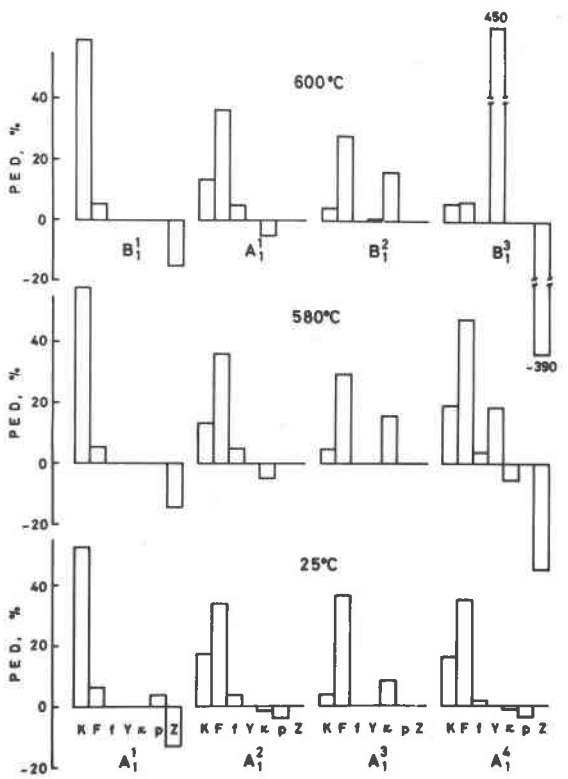

Fig. 1. Contribution (percent) of potential terms in the theoretical frequencies of A_1 species of quartz at 25, 580, and 600°C.

Results and discussion

Electronic polarizabilities

The least-squares fit has been carried out to obtain the best fit between the observed and calculated optical mode frequencies by changing the effective charge and six short-range interaction parameters. The electronic polarizability of a silicon ion α_{Si} is assumed to be isotropic and fixed at 0.02Å^3 according to Tessmann *et al.* (1953). The electronic polarizability of an oxygen ion α_O is determined to reproduce the obtained high-frequency dielectric constants. In Table 1 the optical mode frequencies and the high-frequency dielectric constants, $\epsilon^\infty_\perp$ and $\epsilon^\infty_{/\!/}$, are compared with the experimental data at 25, 580, and 600°C. The calculated results for α quartz of Striefler and Barsch (1975) are also listed in Table 1. The obtained model parameters for the best-fitting model are shown in Table 2. The model presented here for α quartz gives considerably improved agreement for the overall optical frequencies and moderately improved agreement for the *TO–LO* splitting for the stretching vibration mode as compared with Striefler and Barsch's RI model and Barron *et al.*'s E3(RI) model. The obtained small effective charge of $-0.349e$ for the oxygen ions apparently confirms the weak ionic bond nature in quartz, and the present value is only a little smaller than the value $-0.472e$ of Striefler and Barsch and is almost the same as the value of $-0.35e$ of Barron *et al.*, in spite of their neglecting the electronic polarizabilities. The obtained electronic polarizabilities $\alpha_{11}(O) = \alpha_{22}(O)$ [designated as $\alpha_\perp(O)$] = 1.37Å^3 and $\alpha_{33}(O)$ [designated as $\alpha_{/\!/}(O)$] = 1.38Å^3 for α quartz are smaller than those of α_O = 1.7Å^3 reported by Tessmann *et al.* (1953).

207cm^{-1} soft mode A_1^4

The contribution of the potential energy term to the potential energy at 25, 580, and 600°C is presented in Figure 1. At 25°C, the strong stretching and repulsive forces, K and F, contribute mainly to the potential energy of the soft mode A_1^4. On the other

Table 3. Experimental and theoretical (PI model) oscillator strength ($\Delta\epsilon$) of quartz at 25, 580, and 600°C

Species		Experimental* 25°C	580°C	Species		600°C	Theoretical 25°C	580°C	600°C
A_{2T}	1	0.66	0.74	A_{2T}	1	0.73	0.096	0.114	0.098
	2	0.11	0.033	B_{2T}	1		0.0005	0.0002	
	3	0.65	1.57	A_{2T}	2	1.58	0.125	0.230	0.255
	4	0.67	0.40	B_{2T}	2		0.132	0.043	
E_T	1	0.01	0.003	E_{2T}	1		0.0005	0.0002	
	2	0.65	0.695	E_{1T}	1	0.695	0.092	0.105	0.099
	3	0.11	0.13	E_{1T}	2	0.145	0.0009	0.002	0.003
	4	0.02	0.01	E_{2T}	2		0.0016	0.0000	
	5	0.83	1.30	E_{1T}	3	1.30	0.194	0.244	0.245
	6	0.33	0.22	E_{2T}	3		0.035	0.009	
	7	0.05		E_{2T}	4		0.022	0.009	
	8	0.0006		E_{1T}	4		0.004	0.0014	0.031

* *Data are from Gervais & Piriou (1975), except the two lowest E modes, which are from Russel & Bell (1967).*

hand, at 600°C, the weak internal rotation force Y and Coulomb interaction part contribute to potential energy in the soft mode A_1^4 and, moreover, the latter contributes negatively. The potential energy of the soft mode A_1^4 at 580°C has the mix character between that at 25° and that at 600°C. The short-range force constant, the "dynamically effective" ionic charge and the "dynamically effective" electronic polarizability at 25°C are only a little different from those at 580 and 600°C. The contribution of the strong stretching repulsive forces to the potential energy, however, decreases in contrast to the increasing contribution of the weak internal rotation force Y. The frequency of the soft mode decreases as a whole by this effect of the short-range interaction part (Iishi and Yamaguchi, 1975). The mode softening is also attributed largely to the Coulomb interaction part, whose effects become negative while softening. The latter effects were found for the first time by considering the electronic polarizability of ions. More detailed explanation of the mode softening of the soft mode, of course, requires explicit inclusion of anharmonic effects. The neglect of anharmonic effects shows the limitations of the present model.

Oscillator strengths and dielectric constants

The infrared-active mode oscillator strengths, which are related to the *TO–LO* splittings, are also evaluated to examine the appropriateness of the normal modes of vibrations and the model parameters determined in the present work. The calculated oscillator strengths are compared with the observed data in Table 3. The magnitude of the calculated oscillator strengths of the present PI model is five or eight times smaller than the experimental values. The theoretical oscillator strength ratios among modes and temperature dependence are, however, in fairly good agreement with the experimental ones.

The theoretical static dielectric constants in the present model are compared with the experimental data (Gervais and Piriou, 1975) and the results of Striefler and Barsch in Table 4. In Table 4 both sides of the Lyddane-Sach-Teller (LST) relation

$$\frac{\epsilon^0}{\epsilon^\infty} = \prod_i \frac{(\omega_{\mathrm{LO}})_i^2}{(\omega_{\mathrm{TO}})_i^2}$$

are also given to check the correctness of the calculated static dielectric constants by using the present PI model. As was expected from the small value of the calculated strengths and the small magnitude of the calculated *TO–LO* mode splittings, the theoretical static dielectric constants are very small compared with the experimental ones. On the other hand, the static dielectric constants calculated by Striefler and Barsch interpret the experimental values better than the present PI model, in spite of their neglecting the electronic polarizability. Their calculated results, however, do not satisfy the LST relation. As is well known, the static dielectric constants are divided into "high-frequency" contribution related to the electronic polarizabilities and "oscillator strengths" contribution related to *TO–LO* splittings. In the case of ϵ^0 of α quartz, for example, the former is 2.415 and the latter is 2.225, respectively. Striefler and Barsch's model neglecting the electronic polarizability necessarily gives the "high-frequency" contribution the value 1.0. Their dielectric constant $\epsilon^0 = 3.94$, therefore, means that the "oscillator strengths" contribu-

Table 4. Experimental and theoretical dielectric constants and both sides of LST relation of α quartz

		Experimental*	Theoretical Present work	S & B**
ϵ^0		4.43	2.71	3.82
ϵ^0		4.64	2.72	3.94
$\prod_i \frac{(\omega_{LO})_i^2}{(\omega_{TO})_i^2}$	E		1.13	1.16
$\prod_i \frac{(\omega_{LO})_i^2}{(\omega_{TO})_i^2}$	A_{2u}	1.91	1.13	1.16
$\epsilon_\perp^0/\epsilon_\perp^\infty$		1.86	1.14	1.65
$\epsilon_\parallel^0/\epsilon_\parallel^\infty$		1.92	1.13	1.63

* *Gervais & Piriou (1975).* ** *Striefler & Barsch (1975).*

Table 5. Theoretical optical mode frequencies* (in cm^{-1}) of quartz at 25, 580, and 600°C based on the SR model

Species		25°C	580°C	Species		600°C
A_1	1	1126.6	1129.3	B_{1T}	1	1138.9
	2	490.2	472.3	A_{1T}	1	439.1
	3	353.0	336.5	B_{1T}	2	341.7
	4	208.9	42.7	B_{1T}	3	30.6
A_{2T}	1	1118.0	1108.2	A_{2T}	1	1116.9
	2	731.9	687.1	B_{2T}	1	682.5
	3	501.6	449.7	A_{2T}	2	452.5
	4	367.7	407.6	B_{2T}	2	411.5
E_T	1	1130.4	1173.9	E_{2T}	1	1058.2
	2	1113.8	1109.3	E_{1T}	1	1117.2
	3	736.6	709.3	E_{1T}	2	716.2
	4	606.5	622.7	E_{2T}	2	598.5
	5	463.6	428.0	E_{1T}	3	426.7
	6	373.3	371.1	E_{2T}	3	365.4
	7	252.7	255.7	E_{2T}	4	248.1
	8	131.0	100.1	E_{1T}	4	97.5

* *Experimental data are shown in Table 1.*

tion in their model amounts to the large value 2.94. This value 2.94 seems too large when we consider the very small magnitude of their calculated *TO–LO* splittings.

According to Szigeti (1949), the infrared polarization term in the static dielectric constant equation contains two factors,

$$\left(\frac{\epsilon^{\infty}+2}{3}\right)^2$$

and s^2, which are not present in Born's equation. The

Table 7. Parameter values of quartz at 25, 580, and 600°C in the best-fitting SR model

Parameter*	25°C	580°C	600°C
K	4.1143	4.1865	3.7872
F	0.6377	0.5850	0.5624
f	0.4099	0.3918	0.3430
Y	0.0000	-0.0003	0.0007
κ	0.2292	0.2516	0.2483
p	0.0002	0.2064	-0.2750
χ**	4.01	5.54	6.55

* *Units are the same to Table 2.* ** *Elastic constants are not included in the quality-of-fit parameter.*

"s" represents the short-range interaction of electronic and atomic displacements, while the factor

$$\left(\frac{\epsilon^{\infty}+2}{3}\right)^2$$

appears because the long-range interaction does not vanish when it receives transverse waves. The large discrepancy between the theoretical static dielectric constants in the present study and the experimental ones might be caused by ignoring these two factors.

Elastic constants

The theoretical optical mode frequencies obtained by the least-squares fit of both the elastic and the optical mode frequencies based on the SR model are listed in Table 5. The theoretical elastic constants are compared with the experimental results in Table 6. The theoretical best-fit short-range parameters are given in Table 7.

Of the various changes in physical properties associated with the α–β quartz phase transition, the most striking occurs in the elastic constants, as is shown in Figure 2 (Yamamoto, 1974). The Jacobian matrix

Table 6. Experimental and theoretical elastic constants (in 10^{10} dyn/cm²) of quartz at 25, 580, and 600°C based on the SR model

	Experimental			Theoretical		
	25°C*	580°C*	600°C**	25°C	580°C	600°C
C_{11}	87.55	61	136	$47.2(A_1) + 33.8(E) = 81.0$	$17.5(A_1) + 41.8(E) = 59.3$	$121.5(A_1) + 42.6(E_2) = 164.1$
C_{33}	106.8	68	124	$64.0(A_1) = 64.0$	$64.8(A_1) = 64.8$	$162.7(A_1) = 162.7$
C_{44}	57.19	28	38.6	$48.6(E) = 48.6$	$28.1(E) = 28.1$	$29.0(E_1) = 29.0$
C_{55}	57.19	28	38.6	$48.6(E') = 48.6$	$28.1(E') = 28.1$	$29.0(E_1') = 29.0$
C_{66}	40.74	47	51.6	$33.8(E') = 33.8$	$41.8(E') = 41.8$	$42.6(E_2') = 42.6$
C_{12}	6.07	-33	33	$47.2(A_1) - 33.8(E) = 13.5$	$17.5(A_1) - 41.8(E) = -24.4$	$121.5(A_1) - 42.6(E_2) = 78.9$
C_{13}	13.3	-8	48	$11.8(A_1) = 11.8$	$3.8(A_1) = 3.8$	$107.2(A_1) = 107.2$
C_{14}	17.25	7		$13.9(E) = 13.9$	$8.4(E) = 8.4$	

* *Atanasoff & Hart (1941).* ** *Kammer et al. (1948).*

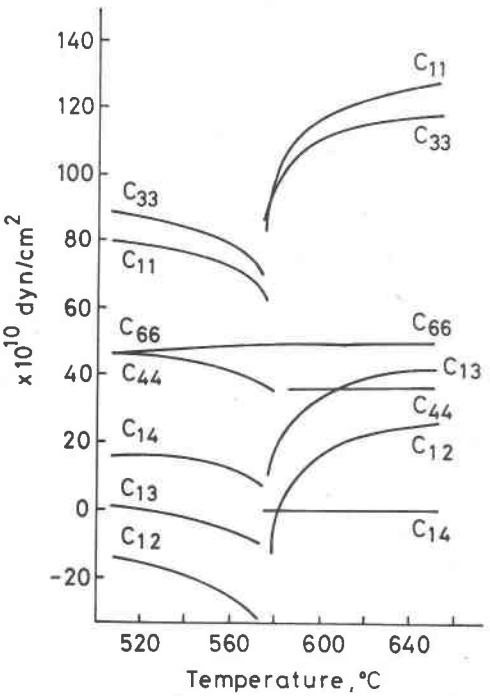

Fig. 2. The temperature dependence of the elastic constants of quartz. Data are from Yamamoto (1974). The elastic constant C_{66} was calculated from the equation of $C_{66} = 1/2(C_{11} - C_{12})$.

elements at 25, 580, and 600°C, *i.e.* the partial derivative of elastic constants with respect to force constants, are listed in Table 8. This table shows that the Jacobian matrix elements of the elastic constants C_{11}, C_{33}, C_{12}, and C_{13} with respect to the internal rotation force Y are extremely large at 580°C. This fact is attributable to the negative elastic constant value of C_{12} and C_{13} and to the decrease of the values of C_{11} and C_{33}, because the internal rotation force is very weak but negative (Table 7) at 580°C.

Table 8. Jacobian matrix elements (in 10^{-3}A^{-1}), *i.e.*, the partial derivatives of elastic constants with respect to force constants of quartz at 25, 580, and 600°C

	C_{11}	C_{33}	C_{44}	C_{66}	C_{12}	C_{13}	C_{14}
25°C							
K	0	0	0	0	0	0	0
F	64	51	57	34	-4	-37	30
f	91	84	14	20	51	77	-15
Y*	1116	1087	509	344	427	915	-417
κ*	4	-14	20	14	-24	13	3
p	1	0	0	0	0	0	0
580°C							
K	0	0	0	0	0	0	0
F	76	100	24	63	-50	-16	20
f	105	107	27	5	95	104	-9
Y*	95573	94514	36346	184	95206	94949	-812
κ*	6	-38	13	10	-14	6	0
p	0	0	0	0	0	0	0
600°C							
K	12	15	0	0	12	14	
F	195	192	20	70	55	85	
f	62	66	29	3	56	63	
Y*	5	1	3721	5	-5	-1	
κ*	-22	-46	15	4	-30	-10	
p	38	44	0	0	38	41	

* *Units of Y and κ are in 10^{-3}Å^{-3}.*

Table 9. Contribution (percent) of potential terms to the theoretical elastic constants of quartz at 25, 580, and 600°C

	C_{11}	C_{33}	C_{44}	C_{66}	C_{12}	C_{13}	C_{14}
25°C							
K	1.7	0.5	4.2	0.9	6.0	5.0	2.8
F	50.8	50.5	74.6	65.0	-20.4	-198.8	137.5
f	46.4	53.8	11.6	24.8	154.6	268.7	-45.1
Y	0.0	0.0	0.0	0.0	0.0	0.0	0.0
κ	1.1	-4.9	9.6	9.3	-40.2	25.0	4.8
p	0.0	0.0	0.0	0.0	0.0	0.0	0.0
580°C							
K	1.4	0.2	5.6	1.9	3.2	-1.4	4.5
F	75.1	90.4	50.9	88.2	120.1	-256.2	137.8
f	69.9	64.9	37.4	5.0	-153.0	1081.6	-44.1
Y	-48.4	-43.7	-3.9	-0.1	117.2	-757.1	2.9
κ	1.9	-11.8	10.3	5.0	12.5	33.4	-1.0
p	0.0	0.0	-0.3	0.0	0.0	-0.2	-0.1
600°C							
K	29.7	34.1	4.7	2.4	59.1	48.0	
F	67.0	66.4	38.1	92.9	39.2	44.8	
f	13.0	13.9	34.7	2.4	24.4	20.0	
Y	0.0	0.0	9.0	0.0	0.0	0.0	
κ	-3.4	-7.0	13.2	2.4	-9.6	-2.4	
p	-6.4	-7.4	0.3	-0.1	-13.1	-10.5	

The contribution of all the potential terms to the calculated elastic constants $(\mathrm{PED})^{\mathrm{E}}_{ij,h}$ is shown in Table 9. The O···O repulsive force F and the Si–Si interaction force f contribute mainly to the elastic constants C_{11}, C_{33}, C_{12}, and C_{13} at 25 and 580°C. On the other hand, the strong Si–O stretching force K contributes considerably to them in addition to the repulsive force F at 600°C. The particular behavior of the elastic constants C_{11}, C_{33}, C_{12}, and C_{13}, which

Table 10. Change of internal coordinates (in Å^3/mdyn)* due to elastic stress of quartz at 25, 580, and 600°C

	S_{xx}		S_{yy}		S_{zz}	S_{yz}	S_{xz}	S_{xy}
	A_1	E	A_1	E	A_1	E	E'	E'
25°C								
Si-O	3	0	3	0	2	7	3	5
O-O	13	-33	13	33	34	-24	42	15
Si-Si	54	-10	54	10	71	32	57	-97
Torsion	128	-64	128	64	168	137	-244	285
580°C								
Si-O	0	1	0	-1	1	12	4	5
O-O	-17	-93	-17	93	-48	18	4	40
Si-Si	118	2	118	-2	89	-86	143	-40
Torsion	2207	6	2207	-6	1636	56	-1124	177
	A_1	E_2	A_1	E_2	A_1	E_1	E'_1	E'_2
600°C								
Si-O	13	0	13	0	19	5	0	6
O-O	45	-51	45	51	23	58	-26	40
Si-Si	23	-7	23	7	32	-111	111	-16
Torsion	2	11	2	-11	-5	-73	-1016	5

* *Units of torsion coordinates are in rad·Å^2/mdyn.*

decrease critically at the transition point and increase rapidly in the β phases (see Fig. 2), is attributed to this large change of the contribution of the potential terms to the elastic constants. The contribution of the potential terms to the elastic constants C_{44} and C_{66}, on the other hand, is always almost the same. Both elastic constants vary only a little through the phase transformation, as is also shown in Figure 2.

Table 10 shows the change in the internal coordinates due to unit elastic stress of quartz. Except in the E mode the internal rotation coordinate becomes surprisingly sensitive to the S_{xx}, S_{yy}, S_{zz}, and S_{xz} stresses at 580°C. The internal rotation coordinates at 600°C are sensitive only to the stress S_{xz}. There is a large variation of the thermal expansion coefficient in the vicinity of the transition point (Fig. 4 of Yamamoto, 1974). This variation may bring about the stress in the quartz structure near the transition point. We conclude now that the sensitive phase transition between the α phase and the β phase is caused through the sensitive E_1' mode internal rotation coordinates due to stress S_{xz}.

Acknowledgments

The author thanks Professor Dr. E. Eberhard for financial support and for the use of the computer in the regional Rechen-Zentrum für Niedersachsen in Hannover, and the Alexander von Humboldt-Foundation for a fellowship. He also wishes to thank Dr. Y. Shiro and Dr. A. Yamamoto of Hiroshima University for providing a computer program.

References

Atanasoff, J. V. and P. J. Hart (1941) Dynamical determination of the elastic constant and their temperature coefficients for quartz. *Phys. Rev., 59,* 85–96.

Axe, J. D. and G. Shirane (1970) Study of the α–β quartz phase transformation by inelastic neutron scattering. *Phys. Rev., B1,* 342–348.

Barron, T. H. K., C. C. Huang and A. Pasternak (1976) Interatomic forces and lattice dynamics of α-quartz. *J. Phys. (C), 9,* 3925–3940.

Bates, J. B. and A. S. Quist (1972) Polarized Raman spectra of β-quartz. *J. Chem. Phys., 56,* 1528–1533.

Bechmann, R. (1958) Elastic and piezoelectric constants of alpha-quartz. *Phys. Rev., 110,* 1060–1061.

Born, M. and K. Huang (1954) *Dynamical Theory of Crystals Lattices, Chap. 5.* Oxford University Press, London.

Chen, S. H. (1967) Group-theoretical analysis of lattice vibrations in metallic β-Sn. *Phys. Rev., 163,* 532–546.

Elcombe, M. M. (1967) Some aspects of the lattice dynamics of quartz. *Proc. Phys. Soc., 91,* 947–958.

Ewald, P. P. (1921) Die Berechnung optischer und elektrostatischer Gitterpotentiale. *Ann. Physik, 64,* 253–287.

Gervais, F. and B. Piriou (1975) Temperature dependence of transverse and longitudinal optic modes in the α and β phases of quartz. *Phys. Rev., B11,* 3944–3950.

Höchli, U. T. and J. F. Scott (1971) Displacement parameter, soft-mode frequency, and fluctuations in quartz below its α–β phase transition. *Phys. Rev. Lett., 26,* 1627–1629.

Iishi, K. and H. Yamaguchi (1975) Study of the force field and the vibrational normal modes in the α–β quartz phase transition. *Am. Mineral., 60,* 907–912.

——— (1976) The analysis of the phonon spectrum of α quartz based on a polarizable ion model. *Z. Kristallogr., 144,* 289–303.

Jay, A. H. (1933) The thermal expansion of quartz by X-ray measurements. *Proc. Roy. Soc., A142,* 237–247.

Kammer, E. W., T. E. Pardue and H. F. Friessel (1948) A determination of the elastic constants for beta-quartz. *J. Appl. Phys., 19,* 265–270.

Russel, E. E. and E. E. Bell (1967) Measurement of the optical constants of crystal quartz in the far infrared with the asymmetric Fourier-transform method. *J. Opt. Soc. Am., 57,* 341–348.

Scott, J. F. (1968) Evidence of coupling between one- and two-phonon excitation in quartz. *Phys. Rev. Lett., 21,* 907–910.

——— and S. P. S. Porto (1967) Longitudinal and transverse optical lattice vibrations in quartz. *Phys. Rev., 161,* 903–910.

Shimanouchi, T. (1963) Force constants of small molecules. *Pure Appl. Chem., 7,* 131–145.

Shiro, Y. and T. Miyazawa (1971) A general matrix method for treating elastic constants of molecular crystals; Application to orthorhombic polyethylene. *Bull. Chem. Soc. Japan, 44,* 2371–2378.

Striefler, M. E. and G. R. Barsch (1975) Lattice dynamics of α-quartz. *Phys. Rev., B12,* 4553–4566.

Szigeti, B. (1949) Polarizability and dielectric constant of ionic crystals. *Trans. Farad. Soc., 45,* 155–166.

Tessmann, J. R., A. H. Kahn and W. Shockley (1953) Electronic polarizabilities of ions in crystals. *Phys. Rev., 92,* 890–895.

Yamamoto, A. (1974) Lattice-dynamical theory of structural phase transition in quartz. *J. Phys. Soc. Japan, 37,* 797–808.

———, Y. Shiro and H. Murata (1974a) Optically-active vibrations and elastic constants of calcite and aragonite. *Bull. Chem. Soc. Japan, 47,* 265–273.

———, ——— and ——— (1974b) The optically-active vibration and elastic constant of soda-niter. *Bull. Chem. Soc. Japan, 47,* 1105–1112.

———, T. Utida, H. Murata and Y. Shiro (1976) Coulomb interactions and optically-active vibrations of ionic crystals—I Theory and application to $NaNO_3$. *J. Phys. Chem. Solids, 37,* 693–698.

Young, R. A. (1962) Mechanism of the phase transition in quartz. *AFOSR-2569 (Final Report, Project No. A-447) Engineering Experimental Station, Georgia Institute of Technology.*

Manuscript received, November 22, 1977; accepted for publication, May 17, 1978.